IOP Conf. Series: Materials Science and Engineering **418** (2018) 012080 doi:10.1088/1757-899X/418/1/012080

Fracture characterization of AHSS using two different experimental methods

G. Huang[1], K. Tihay[2], S. Sriram[1], B. Weber[2], P. Dietsch[2], D. Cornette[2]

[1] ArcelorMittal Global R&D - East Chicago, 3001 E. Columbus Dr., East Chicago, IN 46312, USA
[2] ArcelorMittal Global R&D - Maizières, 57283 Maizières-lès-Metz Cedex, France

gang.huang@arcelormittal.com

Abstract. This paper documents two different methods to characterize the fracture strains of advanced high strength steels (AHSS) under varied stress states to construct the fracture locus. One experimental method is through the strain measurement using Digital Image Correlation, the other method being via thickness reduction measurement. Two AHSS were characterized to determine the fracture loci using the two different methods. The advantages and limitations for both methods are discussed by the analysis of the measured fracture data. Meanwhile, LS-DYNA MAT_224 (*MAT_TABULATED_JOHNSON_COOK) material cards were determined based on the obtained fracture loci and optimized internal parameters, and the cards were applied to predict the fracture behavior of 3-point bending crash tests on the hat-section beam made of the two AHSS. Built upon the discussions on the testing and simulation results, a practice is recommended to improve the accuracy of fracture characterization and prediction.

1. Introduction

The last decade has witnessed a significant increase of AHSS usage in the automotive industry. Application of AHSS enables the automakers to reach their light-weighting goal, in their efforts to satisfy the requirement of fuel efficiency and environment regulations. To address these issues, steel suppliers are continuing to develop products with higher strength and ductility for ease of manufacturability and still retain enough residual ductility for crash energy management. One particularly innovative steel grade, USIBOR®, developed by ArcelorMittal, belongs to a class of products that are tailored to be stamped at elevated temperatures and then quenched in the die to achieve a fully martensitic microstructure. These products are very effective in obtaining complex part shapes coupled with ultra-high strength (up to 2000 MPa) in the part without creating the problem of springback. Furthermore, USIBOR® is coated with aluminum and silicon which result in a scale-free surface of the formed product after hot stamping. These product features make USIBOR® an attractive steel product to be used in automotive body structures.

Due to the trade-off between strength and ductility for conventional steels (including AHSS), application of AHSS has been facing a great challenge to improve the crashworthiness or crash safety performance. Therefore, fracture prediction of AHSS during crash becomes crucial even at the vehicle design stage. For this purpose, several fracture models, such as GISSMO, MIT fracture models and Johnson-Cook model, have been implemented in different material models from LS-DYNA [1], and validation of these fracture models has been documented in the literature [2-9]. While the different

fracture models can be used to predict the fracture moment and location with some degree of confidence, the accuracy still relies heavily on the experimental data as input. The common feature of most of the fracture models implemented in LS-DYNA is that the fracture strain as a function of stress state (stress triaxiality) needs to be supplied to the material input deck, especially for the plane stress loading condition. Consequently, accurate determination of fracture strains from stress states is essential to generate a reliable material card and achieve good accuracy of fracture prediction.

Different methods have been used to determine fracture strains for AHSS. One of the popular measurement techniques is digital image correlation (DIC). As an effectively non-contact technique which can provide the result of the full-field surface strain, it has been widely applied to measure plastic deformation of steels [10,11]. However, since it requires an unobstructed view for image acquisition of the surface where strains are to be measured, the application of DIC technique is very limited for measurement of the deformation of the parts manufactured in the press shop. Thickness measurement is another method which is conventionally used to determine the forming strain and has recently been effectively used to measure the fracture strain [8,9], and it has been extensively applied to the press shop due to its simplicity and promptness in delivering results. The most obvious drawback of the thickness measurement method is that it may significantly rely on users' experience. Other than DIC and thickness measurement, an alternate approach is the hybrid method based on finite element analysis (FEA) and experimental data, which uses FEA to inversely determine the fracture strain upon the good correlation of the global responses (such as load versus displacement) between FEA and experimental data. Even though it does not utilize direct experimental measurement, the hybrid method has been increasingly used for fracture strain determination.

In this paper, the fracture characterization of USIBOR®1500 and USIBOR®2000 is presented. The fracture strain measurement using DIC and thickness reduction is described for different stress states. Meanwhile, the hybrid method is also introduced for some stress states. The LS-DYNA material cards were derived from the facture loci based on the fracture strains measured using DIC and thickness reduction, and were applied to predict the fracture of the component level crash tests on the two USIBOR® materials.

2. Experimental methods

Both USIBOR® materials were die quenched and paint baked at 170 °C for 20 minutes. The tensile properties are shown in Table 1, which were determined from tensile testing based on ASTM E8.

Table 1. Tensile properties of USIBOR® material for fracture testing.

Material	Gauge (mm)	Yield Strength (MPa)	Tensile Strength (MPa)	Uniform Elongation (%)	Total Elongation (%)
USIBOR®1500	1.2	1241	1528	4	6.6
USIBOR®2000	1.6	1549	1883	4.2	6.5

The fracture characterization was carried out using 8 different tests, as summarized in Table 2. The stress states corresponding to the individual tests ranged from shear, uniaxial, plane strain up to equibiaxial stretching (with increasing stress triaxiality). The fracture strains from different tests were measured using DIC and thickness reduction. In addition, the hybrid method was independently applied for purpose of comparison. Tests were conducted in the transverse direction, and the AlSi coating on one side was removed before tests to retain the speckle patterns for the strain measurement using DIC.

2.1. Uniaxial tensile tests

Two types of uniaxial tensile specimens were used. One was according to ASTM E8, and the other followed MatFEM testing method [12].

2.1.1 *ASTM tensile test*. This type of tensile testing was conducted according to ASTM E8 with the DIC system [13]. Due to the high strain concentration, it is noteworthy that the fracture strain could be

significantly dependent on the virtual gauge length defined for the measurement, and the measured fracture strain might be also affected by the velocity of the test and image frame rate.

Table 2. Fracture characterization tests and the applied strain measurement methods.

Name	Uniaxial tensile	Uniaxial - 2	Dome test	Notch tensile	Equibiaxial	Shear Test	VDA	Cut-out test
Stress state	Uniaxial tensile	Uniaxial tensile	Plane strain	Plane strain	Equibiaxial stretch	Shear	Plane strain-2	Drawing
Schematic			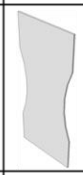		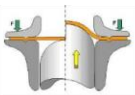		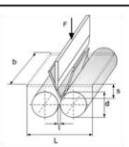	
Strain measurement	DIC	DIC Thickness Reduction	DIC	DIC Thickness Reduction	DIC Thickness Reduction	DIC	Hybrid method	DIC Thickness Reduction

2.1.2. *Tensile tests on specimens with hole*. The specimen of this type of test is similar to that of the tensile test except that it has a center hole. To create the ideal edge quality of the hole to prevent the premature failure of edge cracking, the hole was machined with Electric Discharge Machining (EDM). The fracture strain was determined by measuring the thickness reduction at the broken cross section using an optical microscope or a point micrometer as illustrated in Figure 1 or by DIC.

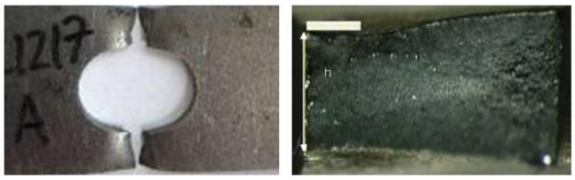

Figure 1. Fracture strain measurement on the center-hole tensile specimen

The local failure strain is directly derived from Equation (1) where h_0 is the initial thickness and h is the reduced thickness at the failure position (assuming isotropic condition):

$$\varepsilon_{\mathrm{eq}} = 2\ln\left(\frac{\boldsymbol{h_0}}{\boldsymbol{h}}\right) \quad (1)$$

2.2. Plane strain tests

Three types of plane strain tests were used in the fracture characterization: notched tensile test, dome test on notched specimen, and V-bending test.

2.2.1. Notched tensile test. The schematic of the notched tensile specimen is illustrated in Table 2. The fracture strain is measured using DIC and thickness reduction at the broken cross section as illustrated in Figure 2, where the local fracture strain is directly derived from final and initial thickness ratio, using

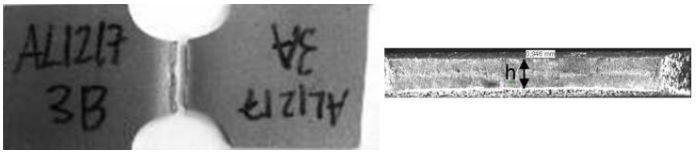

Figure 2. Strain measurement on notch tensile specimen with optical microscope.

$$\varepsilon_{eq} = \frac{2}{\sqrt{3}}\ln\left(\frac{h_0}{h}\right) \quad (2)$$

2.2.2. Dome test. The Nakajima testing method was applied to conduct the plane strain tests. The schematic of the specimen is shown in Table 2. The homogeneous strain field and low strain rate

evolution allow the strain measurement by DIC. It was found that this test has low dependency on the gauge length or grid size adopted for the strain measurement.

2.2.3. V-bending test. The VDA-238 V-bending test [14] consists of applying a load on a wide and sharp punch to deflect a flat specimen supported by two rolling cylinders. This test provides the advantage of avoiding instability effects and it can represent the fracture caused by a local buckling which occurs in structural part under crash load.

Due to the strain gradient through the thickness, the fracture strain cannot be derived from thickness reduction measurement. Figure 3 illustrates how the fracture strain value is obtained from the FEA hybrid method. The strain at failure is determined at the outer fiber of the bending sample. The displacement used in the calculation corresponds to the one measured experimentally at the occurrence of failure.

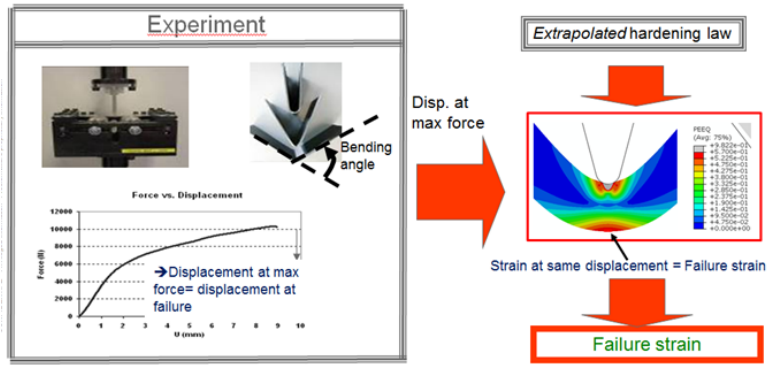

Figure 3. The schematic of hybrid experiment / FEA method for determination of fracture strain in plane strain condition [8]

2.3. Equibiaxial test

Nakajima testing method was used to conduct the equibiaxial tests [16]. Similar to uniaxial tensile condition, the fracture strain can be also derived from thickness reduction at the failure location, as shown in Equation (3).

$$\varepsilon_{eq} = \ln\left(\frac{h_0}{h}\right) \tag{3}$$

2.4. Cut-out tensile test

The cut-out tensile test is similar to the notched tensile test, except that the specimen was designed with a new ratio of radius to width such that its stress state is between the uniaxial tensile and plane strain. In this study, both thickness reduction and DIC were employed to measure the fracture strain. The schematic of the specimen is shown in Table 2.

2.5. Shear test with Smiley specimen

The "Smiley" specimen has been often used to determine the fracture behavior of AHSS under shear condition [17]. The schematic of the specimen is shown in Table 2. Even though there is a possible occurrence of edge cracking, caution was taken to use appropriate dimensions to avoid fracture initiation from the edge. For lack of the deformation in the thickness direction, only DIC was applied to measure fracture strain.

3. Results of fracture characterization

DIC was used to measure the fracture strain for all different tests except the v-bending test. In order to investigate the gauge length effect on the fracture strain measurement, different gauge lengths were applied. For comparison, thickness reduction was used for the uniaxial, plane strain and equibiaxial test, while the hybrid method was used for v-bending test.

3.1. Result from uniaxial tensile tests

The effective fracture strains from ASTM tensile tests were measured using DIC, where three gauge lengths, 0.5, 1 and 2 mm were used. The result is summarized in Figure 4. It is obvious that for both USIBOR® materials, gauge length has a noticeable effect on the fracture strain.

For the tensile tests on the center-hole specimens, both DIC and thickness reduction were applied to measure the effective fracture strains which are shown in Figure 5. It is obvious that the thickness

reduction method gave a fracture strain significantly higher than from DIC method. In the meantime, the data also revealed that the fracture strain had a clear dependency on the gauge length. On the other hand, from the fracture strain comparison in Figures 4 and 5, the difference of fracture strain between USIBOR®1500 and USIBOR®2000 is over 80% and 12%, respectively, using thickness reduction and DIC (on average), in contrast with very similar elongations (total and uniform elongations) shown in Table 1. This implies that the ductility derived from tensile properties does not necessarily represent the fracture properties which need to be determined from the critical area (with fracture initiation) locally.

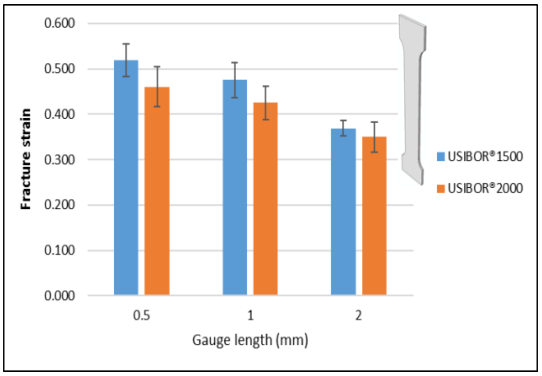

Figure 4. Fracture strains from ASTM tensile tests (DIC)

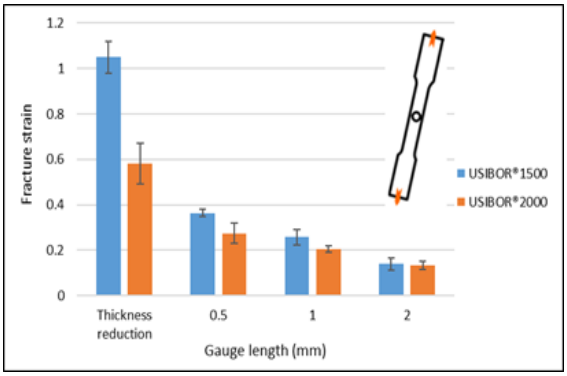

Figure 5. Fracture strains from centre-hole tensile tests (DIC and thickness reduction)

3.2. Result from plane strain tests

Three types of plane strain tests were conducted: tensile tests on notched specimens, dome tests on notched specimen and VDA tests. Both thickness-reduction and DIC were used for fracture strain measurement for notched tensile tests, while only DIC and hybrid method were used to determine the fracture strain for dome tests and VDA tests, respectively. The results of fracture strain are shown in Figures 6-8 for the three types of tests. As described in Figure 6, the fracture strain measured from thickness reduction is more than double that from DIC, which exhibits a trend close to the result from the center-hole tensile tests. However, different from center-hole tensile tests, the gauge length seems to have much less effect on the fracture strain determined using DIC. The result from plane strain dome tests gave a similar trend in terms of the effect of gauge length on the fracture strain, as shown in Figure 7. Figure 8 illustrates the comparison of fracture strains determined from notch tensile tests and VDA tests; a good agreement between the data from two types of tests was reached.

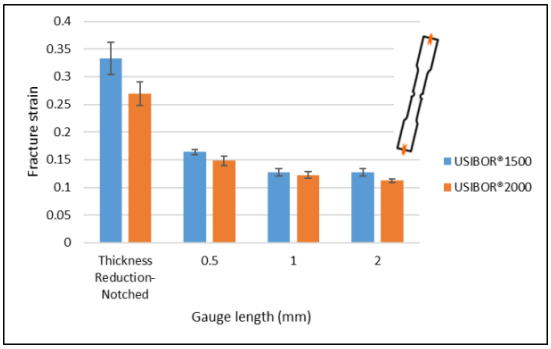

Figure 6. Fracture strains from notched tensile tests (DIC and thickness reduction)

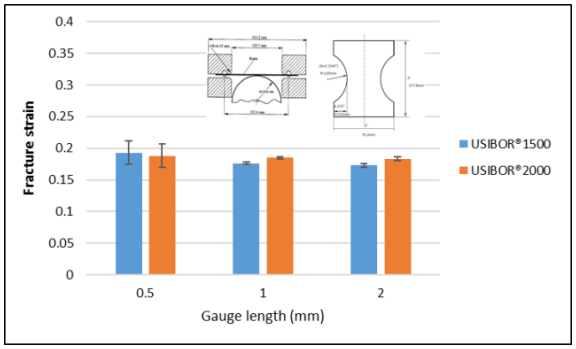

Figure 7. Fracture strains from plane strain dome tests (DIC)

The results from 3 types of plane strain tests demonstrated that the DIC method gave rise to a very similar fracture strain for USIBOR®1500 and USIBOR®2000, while thickness reduction or hybrid method did differentiate the values for the two materials (with a relative difference of over 12%). Furthermore, the fracture strain using thickness reduction is nearly twice that from DIC.

3.3 Result from equibiaxial tests

Figure 9 shows the results from equibiaxial stretch tests using both thickness reduction and DIC. Similar to plane strain tests, the gauge length dependence of the fracture strain was insignificant.

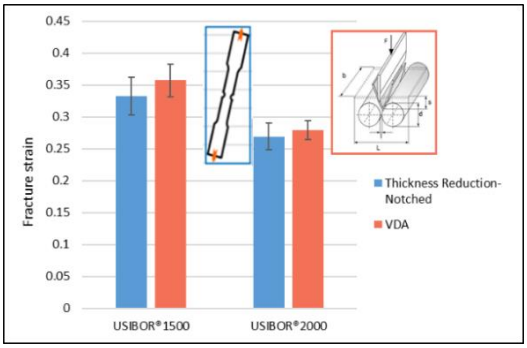

Figure 8. Fracture strains from VDA & compared to notched tensile tests (thickness reduction)

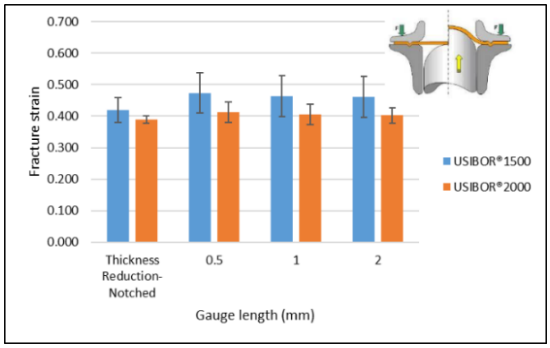

Figure 9. Fracture strains from equibiaxial tests (DIC and thickness reduction)

However, in contrast with plane strain tests, equibiaxial tests gave fairly similar fracture strain resulting from two different measurement methods.

3.4 Result from shear and cut-out tests

The fracture strain results from shear tests and cut-out tests (on specimens with large notches) are shown in Figures 10 and 11, respectively. When applying DIC, due to the small size of the specimen in the critical area (of fracture initiation), only gauge lengths of 0.5 and 1 mm were used for the shear test while only 2 mm gauge length was used for the cut-out test. It can be seen that, USIBOR®1500 exhibited higher fracture strain than USIBOR®2000. The results of cut-out tests also showed that the thickness reduction measurement gave a fracture strain significantly higher than that from DIC.

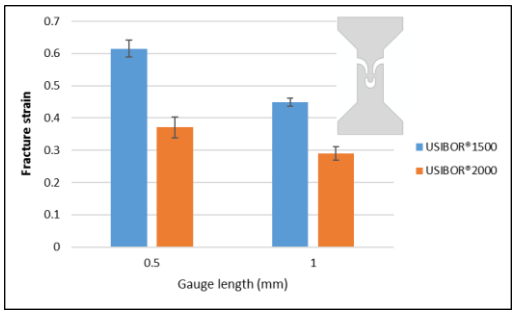

Figure 10. Fracture strains from shear tests (DIC)

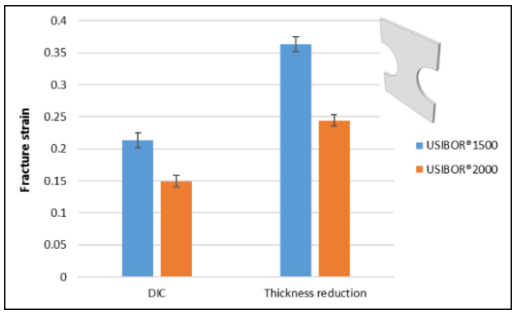

Figure 11. Fracture strains from cut-out tests (DIC and thickness reduction)

4. Fracture prediction on component level test

With the fracture strains determined as a function of stress states, the data were transformed to the material cards following the MAT_224 material model from LS-DYNA, and then were evaluated through fracture prediction of both USIBOR® materials. The component level tests, the 3-point bending tests, were carried out at 8m/s with a mass of 370kg by employing the drop tower. Different crushing distances were applied to determine the first failure occurrence. Numerical simulations were performed with LS-DYNA software [1] by using fully integrated shell elements of 3 mm mesh size with 5 integration layers through the thickness to model the specimen (Figure 12).

4.1. Fracture prediction based on failure curve determined with thickness reduction method

Since only the thinning strain was directly measured after tests, strain ratio (α) of minor strain to major strain was assumed for different tests to calculate the stress triaxiality based on the flow rule, as shown in Equation (4), while triaxiality in MAT_224 was defined with opposite sign [1].

$$\eta = \frac{1+\alpha}{\sqrt{3(1+\alpha+\alpha^2)}} \quad (4)$$

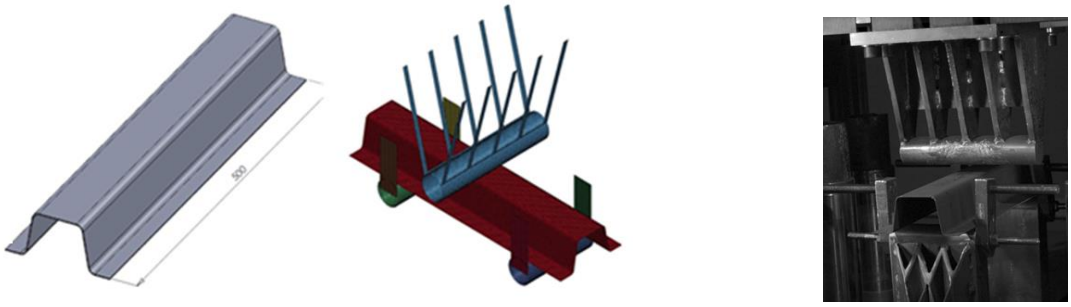

(a) (b) (c)

Figure 12. FEA model and experimental setup for 3-point bending test (a) Schematic of hat-section testing specimen. (b) FEA model of the test. (c) 3-point bending test on the hat-section beam with impacting ram.

The failure curves of both USIBOR® materials were then constructed following the format of MAT_224 model based on the experimental points, as shown in Figure 13 (a), where the modified Mohr-Coulomb model was applied to fit the experimental data [4]. For comparison, Figure 13 (b) delineates the fracture loci using DIC method.

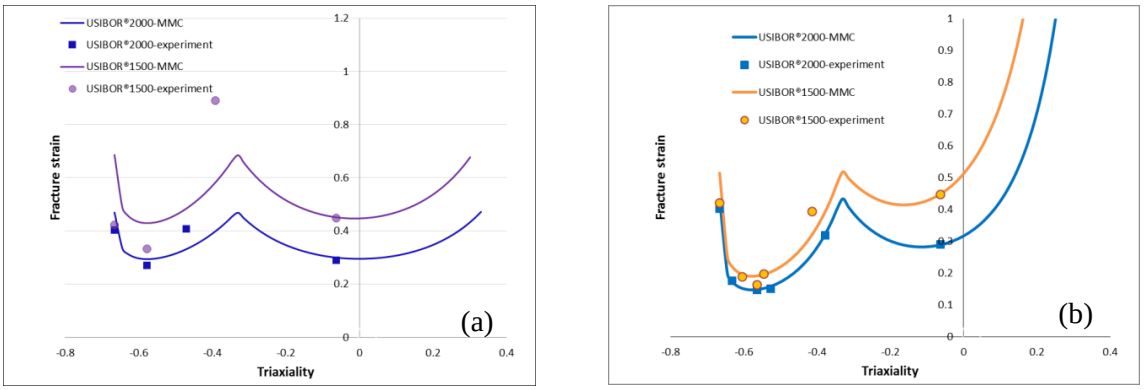

Figure 13. Fracture loci for MAT_224 based on (a) thickness reduction or (b) DIC measurements

Table 3. Fracture prediction of Usibor®1500 & 2000, MAT_224 (with thickness reduction method)

Usibor®1500		
	Crush distance = 94mm	Crush distance = 120mm
		
Usibor®2000		
	Crush distance = 47mm	Crush distance = 120mm
		

From the LS-DYNA material model, the numerical parameter named "NUMINT" allows for tuning sensitivity of fracture initiation. This internal parameter corresponds to the number (or the percentage if the value is negative) of integration points that should satisfy the failure criterion for the deletion. As a first assumption, NUMINT was set to 4; namely, the failure of an element occurs when one entire layer of integration points reaches the failure limit with 5 integration layers.

The fracture prediction in comparison with experiment is shown in the Table 3. For USIBOR®1500, the fracture initiation and propagation were well predicted with a NUMINT value of 4. For USIBOR®2000, the fracture initiation was predicted while at a higher crushing distance, the second crack at the center of the outer hinge below the fold was not predicted.

4.2. Fracture prediction based on failure curve determined with DIC method

Fracture strains for different stress states (triaxialities) were also measured using DIC method. Correspondingly, MAT224 fracture loci denoted by fracture strain as a function of triaxiality were generated based on the failure data from DIC measurement, as shown in Figure 13(b).

As the DIC method led to lower fracture strains compared with the data from the thickness reduction method, a higher percentage of shell element layers that must fail before deletion of the element was used for the parameter NUMINT in MAT224 material cards. In contrast to the material card based on the thickness reduction method, 40-60% for failure of layers was designated (NUMINT = -40 or -60). The LS-DYNA simulation results on the 3-point bending crash tests are provided in Table 4 for Usibor®1500 and Usibor®2000.

Table 4. Fracture prediction of Usibor®1500 & 2000, MAT_224 (fracture strain measured using DIC)

Usibor®1500	Crush distance = 94mm	Crush distance = 120mm
	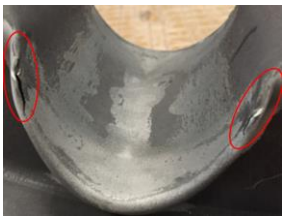 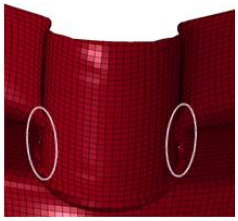	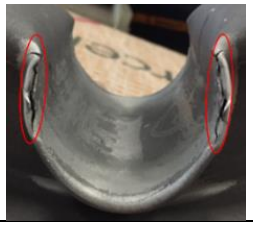 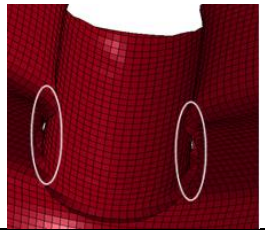
Usibor®2000	Crush distance = 47mm	Crush distance = 120mm
	 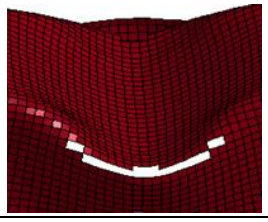	 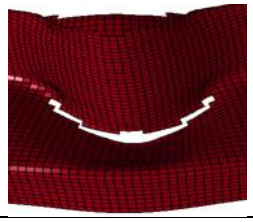

For the simulation result of Usibor®1500 as shown in Table 4, fracture was predicted at the crushing distance of 94 mm except that the severity seemingly was not as high as the test result, even though the moment of 94 mm was assumed to initiate the fracture. Nonetheless, the severity of fracture at 120 mm crushing distance was in good agreement with FEA.

From simulation of Usibor®2000, the result was slightly conservative in terms of prediction of the fracture initiation and propagation. As shown in Table 4, in general the fracture predicted by simulation was more severe than the test result, and the second crack was not well captured either (similar to the case using thickness reduction).

It should be noted that the MAT224 material card for Usibor®2000 was associated with a lower failure percentage (40%) of integration points than for Usibor®1500 (60%), based on the reason that

Usibor®2000 was more sensitive in terms of reaching through-thickness fracture (or deletion of shell element) when bending strain was involved.

5. Discussions and conclusions

During the fracture characterization of the two USIBOR® materials under different stress states (triaxialities), DIC and thickness reduction were used to measure fracture strains which led to the material cards for fracture prediction. Since the introduction of DIC as a non-contact technique for strain measurement, it has been increasingly applied in mechanical characterization including fracture characterization. DIC has been proved to be an effective technique to determine the history of the deformation field and local strain. Even though it is widely used for deformation measurement in the steel and automotive industries, this technique has its intrinsic limitations which need be taken into account when used for measurement of local strain such as fracture strain. As the strain of the last frame of pictures was discretely acquired right before fracture, and considering the high strain rate of AHSS when approaching fracture initiation, the fracture strain could be underestimated. This can be clearly seen from this study. In addition, due to the high strain gradient in the local area encompassing the position of fracture initiation, which was seen for some of the tests in this study, the measured fracture strain could be sensitive to the reference dimension (gauge length).

Thickness reduction has been also often used to measure fracture strain. The advantage of this method is its relative simplicity and its ability to determine the physical fracture strain more conveniently than DIC. Unfortunately, the measure can be impacted by the type of failure (e.g., not applicable for the pure shear case), but also by the acuteness of the operator and the precision of the measurement device (hence a microscope is strongly recommended). On the other hand, since the thickness reduction is conducted after the test and the material is entirely torn apart, the fracture strain might be over-estimated as it is determined at the end of fracture propagation through thickness. Furthermore, although the thickness reduction measurement is independent of or free of gauge length selection, further data are needed for the regularization curve represented by the failure factor as a function of mesh size to construct the fracture material card, for which a method to determine the regularization curve should be developed. Other than the DIC and thickness reduction methods, a hybrid experiment/FEA approach appears as an alternative way to determine the fracture strain in plane strain bending condition. Used under plane strain condition in this paper and when the material has homogeneous mechanical properties through the thickness, the hybrid method can potentially bring an advantage in reducing the uncertainties of the fracture strain measurement.

With the fact that both DIC and thickness reduction have advantages and limitations, after the comparison of the fracture strain data determined using DIC and thickness reduction, a practice is recommended: use the fracture curve measured by DIC as the lower bound and the curve from thickness reduction as the upper bound for the fracture locus to be incorporated into the material card; or the fracture locus should be depicted within the range prescribed by the low limit from DIC (right before fracture initiation) and upper limit from thickness reduction (right after the end of fracture propagation through thickness).

The component-level numerical simulations indicated that irrespective of the different practices to calibrate and generate the failure material card, it is necessary to prescribe properly the internal numerical parameter of the material card (here the parameter NUMINT in LS-DYNA). Meanwhile, it is recommended that vast characterization tests should be conducted to cover a wide range of stress states, in order to have a good combined accuracy of material cards for fracture prediction. It is also recommended to include more validation tests at the component level to generate material cards of higher accuracy.

Acknowledgments
Authors would like to acknowledge the encouragement and support from Jayanth Chintamani, Michel Babbit and Martin Munier. The testing work performed by George Girman, Robert Houser, Cyril Di Vicoli, Virginie Marchal and Frédéric Colli is also highly appreciated. The authors would also like to thank Barbara Banek for the proofreading.

References
[1] LS-DYNA 971 / Rev5 (beta) Keywords Users Manuel Vol I Livermore Software Technology Corp. May 2010, http://lstc.com/pdf/ls-dyna_971_manual_k.pdf
[2] Dell H, Gese H, Oberhofer G 2007 CrachFEM: A comprehensive approach for the prediction of sheet metal forming, *NUMIFORM'07 Materials Processing and Design: Modeling, Simulation and Applications* 18- 21th June 2007 Porto PortugalMore references
[3] Wierzbicki T, Bao Y, Lee Y W, Bai Y 2005 Calibration and evaluation of seven fracture models, *Int. J. of Mech. Sci.* **47** p 719
[4] Bai Y and Wierzbicki T 2010 Application of Extended Mohr-Coulomb Criterion to Ductile Fracture, *Int. J. Frac.* **161** p 1
[5] Johnson G R and Cook W H 1985 Fracture characteristics of three metals subjected to various strains, strain rates, temperature and pressures *Eng. Frac. Mech.* **21** p 31
[6] Basaran M, Wolkerlin S D, Feucht M, Neukamm F, Weichert D An extension of the GISSMO damage model based on lode angle dependence *LS-DYNA Anwenderforum* Bamberg 2010
[7] Huang G, Zhu H, Sriram S, Chen Y, Xia Z C, Faruque O 2014 Fracture prediction and correlation of AlSi hot stamped steels with different models in LS-DYNA *13th International LS-DYNA Users Conference* 2014 Detroit
[8] Dietsch P, Tihay K, Cobo S, Sarkar S, Hasenpouth D, Cornette D 2017 Predictive approach for crash performance of press-hardened steels and its application on new product developments *CHS2 2017 6th International Conference on Hot Sheet Metal Forming of High-Performance Steel* 4-7 June 2017 Atlanta GA USA
[9] Dietsch P, Tihay K, Bui-Van A, Cornette D 2017 Methodology to assess fracture during crash simulation: fracture strain criteria and their calibration *Metall. Res. Technol.* **114**, 607
[10] Sutton M A, Cheng M, Peters W H, Chao Y J and McNeill S R 1986 Application of an optimized digital correlation method to planar deformation analysis *Image and Vision Computing* **4** p 143
[11] Huang G, Yan B and Zhu H 2009 Measurement of fracture strains for advanced high strength steels using digital image correlation *SAE Paper* **09M-1174**
[12] Hooputra H, Gese H Dell H and Werner H 2004 A comprehensive failure model for crashworthiness simulation of aluminum extrusions *Int. J. Crash* **9** p 449
[13] Noncontact Measurement Solutions, www.correlatedsolutions.com
[14] VDA 238-100 Plate bending test for metallic materials *VDA test specifications* 2010
[15] Reynes A, Eriksson M, Lademo O G, Hopperstad O S, Langseth M 2009 Assessment of yield and fracture criteria using shear and bending tests *Material and Design* **30** p 596
[16] Standard testing method for determining forming limit curves **ASTM E2218-15** 2015
[17] Roth C C, Erice B, Effect of strain rate and temperature on ductile fracture: New experiments on AHSS sheets and modelling *MIT ICL Fracture Workshop* October 2015 Boston